ADVANCED MATERIALS INTERFACES

www.advmatinterfaces.de

Adsorption and Exchangeability of Fibronectin and Serum Albumin Protein Corona on Annealed Polyelectrolyte Multilayers and Their Consequences on Cell Adhesion

*Nicolas E. Muzzio, Miguel A. Pasquale, Xabier Rios, Omar Azzaroni, Jordi Llop, and Sergio E. Moya**

Polyelectrolyte multilayers (PEMs) based on biopolyelectrolytes are highly appealing for the surface engineering of biomaterials and the tuning of cell response and phenotypes for biomedical applications. However, cell adhesion is limited on biopolyelectrolyte PEMs. Thermal annealing provides a simple means to increase or decrease cell adhesion on PEMs. The work presented here aims to understand cellular interactions with annealed PEMs based on the adsorption and exchangeability of two model proteins: fibronectin (FN), an adhesion protein, and bovine serum albumin (BSA), a nonadhesion protein. Protein adsorption and exchangeability are studied on annealed poly-L-lysine (PLL)/sodium alginate (Alg) and chitosan (Chi)/hyaluronic acid (HA) PEMs using [^{131}I] radiolabeled proteins and gamma counting. Upon annealing cell adhesion is enhanced on PLL/Alg multilayers and decreased on Chi/HA multilayers. For PLL/Alg PEMs, annealing increases adsorption of both FN and BSA and reduces exchangeability. For Chi/HA multilayers, annealing increases BSA adsorption but decreases FN deposition, accompanied by a greater exchangeability. Changes in topographic features of deposited proteins on annealed PLL/Alg hint on changes in the 3D structure of the proteins. Circular dichroism shows that FN retains a large β-sheet contribution upon adsorption to both annealed and unannealed PLL/Alg PEMs, also suggesting changes in tertiary structure.

1. Introduction

Cell adhesion is a key process in many physiological and pathological processes and a fundamental issue in biomedical fields.[1–5] Controlling the adhesion of cells to the interface of artificial materials is a basic requirement for the development of scaffolds and medical devices. However, the interaction of materials with cells is complex and often poorly understood.[6] It is known that cells adhere to substrates through adhesion proteins present in the cell media and biological fluids, such as fibronectin (FN), which are sensed by integrins from the cell membrane. Adhesion proteins must adhere first to the material's surface and cells will follow. The concentration of adhesion proteins is very small in relation to other proteins present in biological fluids, such as hemoglobin or serum albumin, which compete with adhesion proteins for attachment to surfaces and formation of a "protein corona."[7] Protein conformation should change upon adsorption to different extents based on the protein type and environmental conditions.[8] The attachment and stability of adhesion proteins is highly influenced by the nature of the substrate, including its roughness, surface chemistry, contact angle, and other characteristics, which in turn will play an important role on cell adhesion and growth and on other cell functions such as myogenic differentiation[9] and stem cell differentiation.[10–13]

Polyelectrolyte multilayers (PEMs) are fabricated by the so-called layer-by-layer (LbL) technique. The LbL technique makes use of the alternating assembly of oppositely charged polyelectrolytes led by electrostatic interactions.[14] PEMs made from biopolyelectrolytes are very appealing for tissue engineering as they are biocompatible, easy to assemble on charged surfaces, and can incorporate growth factors or other biomolecules assembled in between the layers or on top of the PEM, which can promote cell adhesion, cell mobility, mineralization, tissue regeneration, and other processes. However, biopolyelectrolyte-based PEMs have weak adhesive properties for cells. Picart and co-workers have shown that chemical crosslinking of PEMs improves cell adhesion. Biopolyelectrolyte PEMs are soft,

Dr. N. E. Muzzio, Dr. S. E. Moya
Soft Matter Nanotechnology Group
CIC biomaGUNE
Paseo Miramón 182, 20014 San Sebastián, Guipúzcoa, Spain
E-mail: smoya@cicbiomagune.es
Dr. M. A. Pasquale, Dr. O. Azzaroni
Instituto de Investigaciones Fisicoquímicas Teóricas y Aplicadas (INIFTA)
Departamento de Química
Facultad de Ciencias Exactas
Universidad Nacional de La Plata
CONICET
Sucursal 4, Casilla de Correo 16, 1900 La Plata, Argentina
X. Rios, Dr. J. Llop
Radiochemistry and Nuclear Imaging Group
CIC biomaGUNE
Paseo Miramón 182, 20014 San Sebastián, Guipúzcoa, Spain
The ORCID identification number(s) for the author(s) of this article can be found under https://doi.org/10.1002/admi.201900008.

DOI: 10.1002/admi.201900008

with an elastic modulus of a few kPa before crosslinking. The improved cellular adhesion is understood to occur as a consequence of the increase in elastic modulus of PEMs following crosslinking.[15–17]

In a series of papers, we have explored the impact of thermal annealing of PEMs on cell adhesion.[18–20] Thermal annealing, exposing PEMs to a specific temperature (usually 37 °C) for periods for 1–3 d, enhanced the adhesion of A549 and C2C12 cells on biocompatible poly-L-lysine (PLL)/alginate (Alg) and PLL/dextran sulfate (Dex) PEMs. The cytoplasm spreading of A549 and C2C12 cells on unannealed PLL/Alg films is poor, while cells seeded on annealed $(PLL/Alg)_7PLL$ PEMs present an extended cytoplasm with well-defined focal contacts and large actin fibers, and the adhesion parameters reaching values statistically equal to the values found for glass. In contrast, we found that annealed chitosan (Chi)/hyaluronic acid (HA) PEMs become less adhesive toward specific cell lines.[19] We observed the adsorption of bovine serum albumin (BSA), a nonadhesion protein, on Chi/HA PEMs by quartz crystal microbalance (QCM-D), but the deposition of adhesion proteins could not be traced as the amount deposited was below the technique's sensitivity limits.[19,20] Indeed, this result hinted that the limited cell adhesion could be related to a scarce adsorption of adhesion proteins onto the PEMs.

Thermal annealing results in the reorganization of PEMs, causing changes in contact angle, surface charge, and mechanical properties.[21] After annealing, the polyelectrolytes rearrange in the multilayers from a stratified organization to molecular complexes of polycations and polyanions, where the interaction between oppositely charged polyelectrolytes is maximized.

In a seminal work, Schlenoff and co-workers suggested that differences in cell adhesion between poly(diallyldimethylammonium chloride)/poly(sodium 4-styrenesulfonate) (PDADMAC/PSS) multilayers of varying thickness and with different surface charge densities are related to the stability of adsorbed proteins on the PEMs.[22] The authors showed that cell adhesion is correlated to the lability of deposited BSA rather than the amount of BSA deposited. Employing radiolabeled BSA, they showed that cells adhere better to PEMs with more stable BSA layers where there is less exchange with proteins from the culture media, and suggested an extrapolation to adhesion proteins. The use of radiolabeled proteins has the advantage of high sensitivity, making them particularly useful for studying competitive protein adsorption since even just a few molecules can be detected by gamma counting.[23] Other authors have radiolabeled adhesion proteins and quantified their deposition on surfaces with variable chemistry, showing that cell adhesion depends on the amount and conformation of adhesion proteins adsorbed.[8,24,25]

We aim here to understand why thermal annealing of multilayers impacts on cells adhesion and why for PLL/Alg PEMs the annealing induces an enhanced adhesion while for Chi/HA PEMs it reduces cell adhesion. We will study how the annealing affects the deposition and exchangeability of FN and BSA as cell adhesive and nonadhesive protein models, respectively. Adsorption and exchangeability studies will be conducted with radiolabeled proteins using gamma counting for protein quantification. Since gamma counting allows to quantify small number of molecules, we will be able to work in concentration of FN as low as in cell media. Moreover, we will study the deposition of radiolabeled FN in presence of nonlabeled BSA and will assess the influence of BSA on the deposition of FN and its exchangeability. To our knowledge, few works have addressed the cooperativity between adhesive and nonadhesive proteins by quantifying protein deposition by gamma counting.[26–28] We will relate the adsorption and exchangeability of FN and BSA to changes in their secondary and tertiary structure when deposited to the annealed PEMs resulting from the different organization of the multilayers after annealing. Overall, our results will provide a deeper understanding of the importance of the deposition and stability of nonadhesive and adhesive proteins on cell adhesion on polyelectrolyte multilayers, which were only partially addressed in previous works or only for BSA.[22] We will address the importance of cooperative interactions between adhesive and nonadhesive proteins and we will demonstrate that observations about the deposition and exchangeability of nonadhesive proteins cannot be necessarily extended to adhesive proteins. Finally, we will show how changes in the organization of multilayers and surface characteristics can affect their interaction with adhesive and nonadhesive proteins and impact on cell adhesion. Understanding how the characteristics of a material or interface affect their interaction with proteins and cells is fundamental for the development of biomaterials with tailored properties and our results can be extrapolated to other materials and interfaces.

2. Results

2.1. Cell Adhesion Characteristics and Substrate Physicochemical Properties

Thermal annealing of biopolyelectrolyte-based PEMs induces changes in their physicochemical properties and morphology with significant consequences for cell adhesion (**Figure 1**). We have shown in previous works that thermal annealing of PLL/Alg PEMs results in an increase in cell adhesion, while the annealing of Chi/HA results in a decrease in cell adhesion. This contrasting cell behavior on annealed PEMs has been observed for different cell lines, including for C2C12 cells, which exhibit this behavior when seeded on the PEMs studied here (n-PLL/Alg, a-PLL/Alg, n-Chi/HA, and a-Chi/HA, Figure 1b,c).[18–20] For PLL/Alg PEMs, thermal annealing increases the Young's modulus of the sample, produces a more hydrophobic surface with a contact angle approaching 90°, enhances the negative charge, and decreases the roughness (Figure 1d).[21] In the case of Chi/HA PEMs, the changes in physicochemical properties are significantly smaller. Thus, the surface remains hydrophilic, with a decrease in the contact angle from 30° to 21°, the charge becomes slightly more negative, and the elastic properties remain unchanged. However, there is a significant change in root mean square (RMS) roughness for a-Chi/HA PEMs compared with n-CHI/HA PEMs. Upon annealing, the RMS of the roughness decreases to half of that measured for unannealed samples. This change in roughness could explain a different interaction of the PEMs with cells after annealing (Figure 1c).[19]

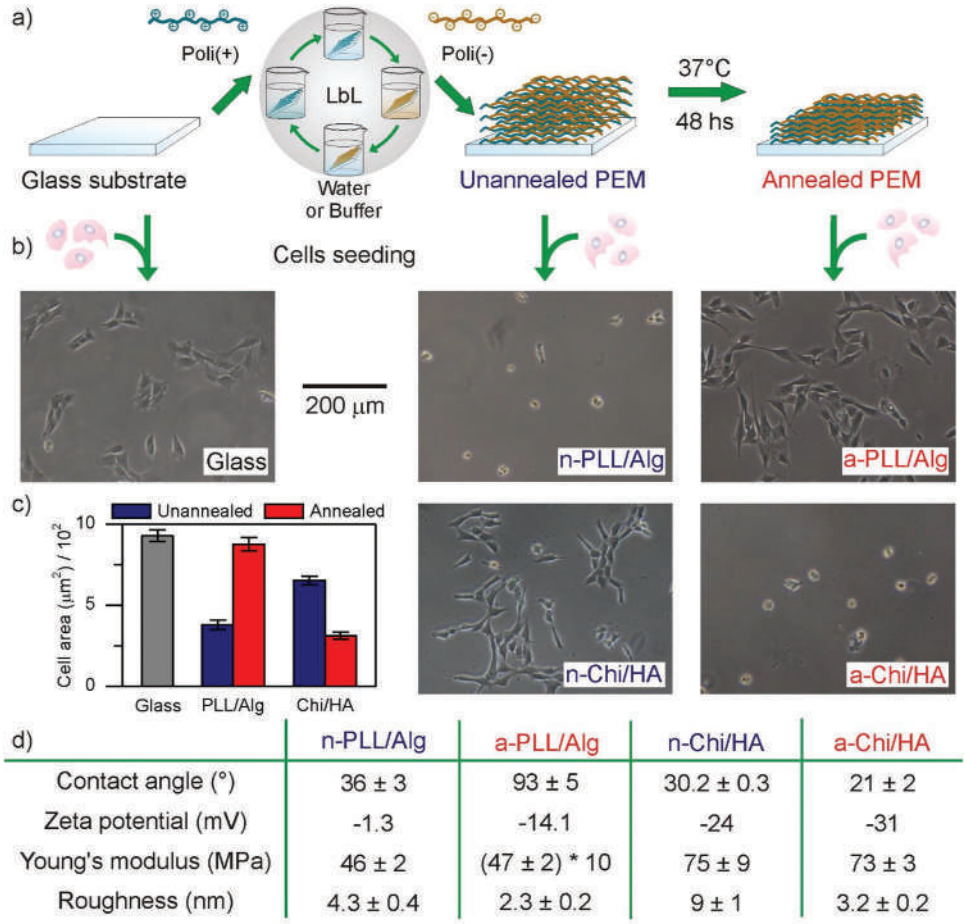

d)	n-PLL/Alg	a-PLL/Alg	n-Chi/HA	a-Chi/HA
Contact angle (°)	36 ± 3	93 ± 5	30.2 ± 0.3	21 ± 2
Zeta potential (mV)	-1.3	-14.1	-24	-31
Young's modulus (MPa)	46 ± 2	(47 ± 2) * 10	75 ± 9	73 ± 3
Roughness (nm)	4.3 ± 0.4	2.3 ± 0.2	9 ± 1	3.2 ± 0.2

Figure 1. Changes in cell adhesion and in the physicochemical properties of PEMs induced by thermal annealing. a) Scheme of the assembly and annealing protocol. b) Phase contrast images of C2C12 cells adhered on glass, n-PLL/Alg, a-PLL/Alg, n-Chi/HA, or a-Chi/HA as indicated. c) Average cell adhesion spreading area from cells seeded on glass, n-PLL/Alg, a-PLL/Alg, n-Chi/HA, or a-Chi/HA PEMs. d) Changes in physicochemical properties of PEMs from our previous work.[18–20]

The spreading area of C2C12 cells on a-PLL/Alg is comparable to that of cells seeded on glass or polystyrene control surfaces. An average value of about 930 µm^2 is obtained from cells seeded on glass or annealed PLL/Alg PEMs (Figure 1c).

Cells seeded on both n-PLL/Alg and a-Chi/HA showed a rounded shape and an average spreading area 60% lower than the value obtained from cells on glass or a-PLL/Alg (Figure 1b,c).

Cells adhered to n-Chi/HA exhibited a significantly smaller cell spreading area and more tapered morphology than on glass. Cell agglomerates with peripheral cells with rather large filopodia in a quasi-stellate morphology. On the other hand, for annealed Chi/HA-based PEMs, C2C12 cells appeared rounded and the average cell spreading area decreased to about 250 µm^2.

2.2. Adsorption and Exchangeability of Adhesion and Nonadhesion Model Proteins by Radiochemistry Assays

The adsorption of BSA and FN proteins and their exchangeability with proteins from the complete culture medium was evaluated on n-PLL/Alg, a-PLL/Alg, n-CHI/HA, and a-CHI/HA PEMs employing radiolabeled [^{131}I]-BSA and [^{131}I]-FN. To study protein exchangeability, PEMs with preadsorbed radiolabeled proteins were exposed for 18 h to either protein-free medium or fetal bovine serum (FBS)-supplemented medium (**Figures 2** and **3**).

For n-PLL/Alg exposed to a 1 mg mL^{-1} [^{131}I]-BSA solution, 12.0 ± 0.2 µg cm^{-2} of BSA was detected on the PEMs (Figure 2a). After incubation in plain or FBS-supplemented Roswell Park Memorial Institute (RPMI) medium for 18 h, the remaining BSA on the PEM decreased to 52 and 23% from the original activity, respectively. Upon annealing, the amount of BSA adsorbed increased to 19 ± 1 µg cm^{-2} and BSA exchangeability decreased (Figure 2a).

On the other hand, the adsorption of FN for 45 min from a 10 µg mL^{-1} solution in 4-(2-hydroxyethyl)-1-piperazineethanesulfonic acid (HEPES), resulted in the deposition of 187 ng cm^{-2} on n-PLL/Alg, more than two orders of magnitude lower than the mass per unit area of BSA adsorbed. The amount of FN diminishes to about 125 and 74 ng cm^{-2} after immersion for 18 h in either plain or FBS-supplemented RPMI media, respectively (Figure 2b). As for the behavior observed for BSA, on a-PLL/Alg the FN exchangeability significantly decreased

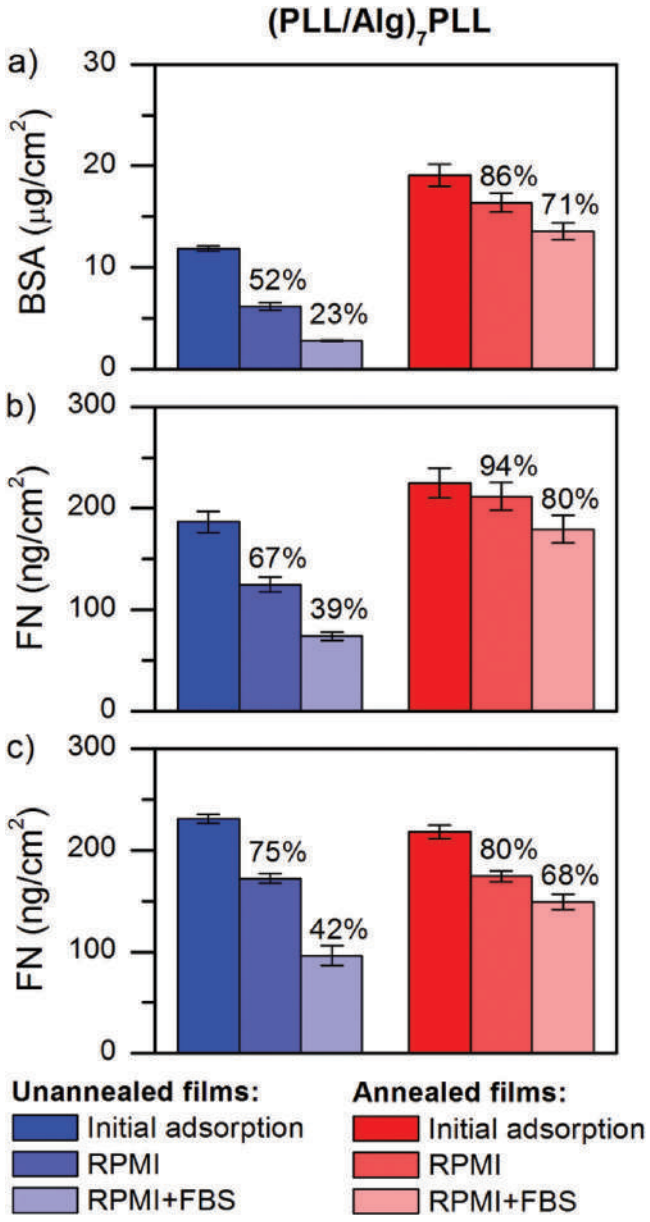

Figure 2. Quantification of the adsorption of [^{131}I] radiolabeled FN and BSA proteins on PLL/Alg PEMs, and determination of exchangeability by gamma counting. The graphs display the amount of FN or BSA adsorbed to unannealed and annealed PLL/Alg PEMs from solutions containing a) 1 mg mL^{-1} BSA, b) 10 μg mL^{-1} FN, or c) 1 mg mL^{-1} BSA and 10 μg mL^{-1} radiolabeled FN. Exchangeability is indicated by the decreases in the amount of adsorbed protein remaining on the PEMs following immersion in plain (RPMI) or complete (RPMI + 10% FBS) culture media. Percentages shown express these decreases relative to the amount of protein on the PEMs from the initial adsorption.

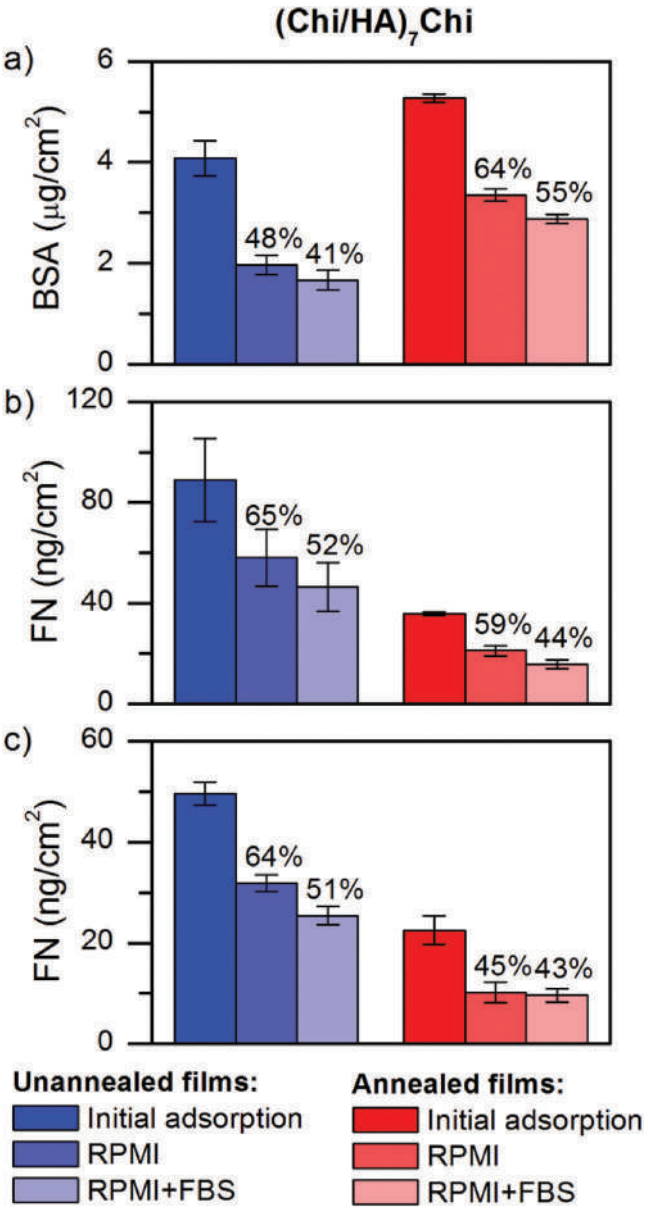

Figure 3. Quantification of the adsorption of radiolabeled FN and BSA proteins on Chi/HA PEMs, and determination of exchangeability by gamma counting. The graphs display the amount of FN or BSA adsorbed to unannealed and annealed Chi/HA PEMs from solutions containing a) 1 mg mL^{-1} BSA, b) 10 μg mL^{-1} FN, or c) 1 mg mL^{-1} BSA and 10 μg mL^{-1} radiolabeled FN. Exchangeability is indicated by the decreases in the amount of adsorbed protein remaining on the PEMs following immersion in plain (RPMI) or complete (RPMI + 10% FBS) culture media. Percentages shown express these decreases relative to the amount of protein on the PEMs from the initial adsorption.

compared with n-PLL/Alg (Figure 2b). Values of FN density on PLL/Alg PEMs are in the order of magnitude of those reported for a FN monolayer, that is, 0.28, 0.40, and 0.32 μg cm^{-2}.[24,25,29]

It has been reported that the charge and chemistry of PEMs, determined by the polyelectrolytes assembled, play a key role in the overall cell behavior on the multilayers.[22] Upon annealing, the surface charge, wettability, topography, and mechanical properties of PLL/Alg PEMs are modified. The annealing induces a reorganization of the polyelectrolyte chains to maximize opposite charge interactions. Despite this reorganization, a-PLL/Alg PEMs become more negative due to the larger molecular weight of Alg relative to PLL, and the exposure of negative carboxylic groups from alginate at the PEM interface. This reorganization process also increases PEM stiffness as

reported in our previous work.[18] It has been shown that FN interacts with cell protein integrins ($\alpha_5\beta_1$) more tightly when adsorbed to surfaces displaying negative moieties, such as carboxyl, sulfonic, or hydroxyl groups, favoring cell adhesion.[30–33] Furthermore, FN adsorbs in a larger amount when the surface wettability decreases.[34] Cell adhesion is also improved when FN adhesion groups are exposed for integrin binding.[24] The more hydrophobic characteristics of the PEM after annealing and the presence of carboxylic groups from Alg would explain the more favorable interaction of FN with the PEMs.

The exchange of preadsorbed FN on both n-PLL/Alg and a-PLL/Alg varies when FN is adsorbed from a solution containing both 1 mg mL^{-1} BSA (non-radiolabeled) and 10 μg mL^{-1} [^{131}I]-FN compared with adsorption from a solution of 10 μg mL^{-1} [^{131}I]-FN only (Figure 2c). First, the adsorbed mass of FN from the FN/BSA solution on n-PLL/Alg reaches a value of about 230 ng cm^{-2}. Concomitant with the increase in FN adsorption, the exchangeability of FN increases, particularly after immersion in FBS-supplemented RPMI medium. Upon annealing, the mass of FN adsorbed on the PEMs from the FN/BSA mixture is similar to the mass adsorbed on n-PLL/Alg from pure FN but the exchangeability results in a similar percentage decrease as that observed for BSA on a-PLL/Alg.

The larger amount of FN adsorbed on PLL/Alg from the FN/BSA solution compared with the FN only solution could be due to a cooperative interaction between BSA (which is present in excess) and FN, which results in better FN adsorption. However, it is worth noting that for a-PLL/Alg, the adsorbed FN from the FN/BSA solution seems to be conditioned by the exchangeability of BSA. This means that BSA, particularly on annealed samples, additionally affects the interaction of FN with the PEMs, or that there is FN associated with BSA but not interacting with the PEM substrate. Thus, BSA, which absorbs in much larger quantities than FN, has an impact on FN adsorption and exchangeability. Although BSA is used to avoid nonspecific adsorption,[35] a "hard corona" of adsorbed BSA allows cell adhesion as has been recently demonstrated for 3T3 fibroblasts.[22] Nevertheless, for both preadsorbed FN from a solution of FN alone and from a solution of FN and BSA, thermal annealing of PLL/Alg PEMs increases the stability of adsorbed FN. Proteins adhere more tightly upon annealing of the PEMs and there is likely a larger amount of arginine-glycine-aspartate (RGD) groups from FN that are able to interact with cell membrane integrins to favor cell adhesion.

For Chi/HA-based PEMs (Figure 3), the amount of BSA or FN deposited on the PEMs is smaller than for PLL/Alg PEMs. The amount of BSA adsorbed on n-Chi/HA is about three times smaller than that observed for n-PLL/Alg, and on a-Chi/HA, the adsorption is about four times smaller than for a-PLL/Alg. Similarly, FN adsorption on n-Chi/HA is approximately half of that observed for n-PLL/Alg, and an even more significant decrease is observed for annealed samples. As for a-PLL/Alg PEMs, after annealing a-Chi/HA exhibits an increased BSA adsorption and a decrease in exchangeability compared with n-Chi/HA (Figure 3a).

For FN adsorbed from a 10 μg mL^{-1} FN solution, there was an adsorption of about 90 ng cm^{-2} on n-Chi/HA and 36 ng cm^{-2} on a-Chi/HA PEMs (Figure 3b). The remaining FN after the exchanges is also much smaller than for PLL/Alg PEMs. The adsorption of FN from the solution with FN and BSA results in a smaller amount of FN deposited on both annealed and unannealed PEMs. This is also different from the PLL/Alg-based PEMs, where the presence of BSA increased the deposition of FN. It is likely that BSA deposits in a different fashion on Chi/HA PEMs, which does not favor the interaction with FN (Figure 3c). A similar exchangeability of FN was observed for FN adsorbed from the FN/BSA solution (Figure 3c) and the FN-only solution (Figure 3b). We thus conclude that thermal annealing reduces the interactions between adhesion proteins and Chi/HA PEMs, the reverse effect of that observed for PLL/Alg PEMs.

These results agree with the antiadhesive characteristics of Chi/HA PEMs for cells and bacteria, which are more apparent after annealing. The number of FN proteins adsorbed from cell culture medium, and the strength of their interaction with the Chi/HA PEM would be smaller than that required for achieving proper cell adhesion characteristics.[36] Chi/HA PEMs, either unannealed or annealed, have been demonstrated to be hydrophilic[19] and as such, deposited proteins can be expected to be labile.[37,38]

Results from protein adsorption and exchangeability assays allow us to rationalize the observed adhesion characteristics of the different cell lines tested in previous works. Cells adhering to a substrate interact with it via proteins from the culture medium that adhere to the substrate first; thus, the nature of the protein/substrate interactions would define the cell adhesion properties. We have demonstrated that physicochemical properties of PEMs change upon annealing.[18–20] In the present work, we show that protein adsorption on either adhesive or nonadhesive substrates exhibits distinctive behavior upon annealing.

PLL/Alg PEMs increase their hydrophobicity upon annealing due to the reorganization of the polyelectrolyte chains in the multilayers to maximize electrostatic interactions of oppositely charged polyelectrolytes, exposing negative groups that would interact with positively charged regions of globally charged negative proteins, such as BSA. The decrease in electrostatic interactions produced during the described process would be compensated by the increase in hydrophobicity of the substrate. It is worth mentioning that roughness appears to not be the most relevant characteristic for cell adhesion on these PEMs as the thermal annealing results in a smoother surface, at least in the scale length measured by atomic force microscopy (AFM). The variation in the amount of adsorbed protein is not expected to be caused by changes in roughness either.

It is a well-known fact that it is not only the amount of adsorbed proteins that plays a key role in cell adhesion, but also the strength of the interaction of the proteins with the substrate and the resulting protein configuration.[22] Protein exchangeability measured with radiolabeled FN and BSA provides insight into the protein adsorption process on PEMs. The simultaneous adsorption of BSA and FN on PLL/Alg indicates that BSA affects FN interaction with the substrate and that this interaction is modulated by the annealing. In both cases, the exchangeability of FN deposited alone or from a solution with BSA, as well as that of BSA protein, decrease on annealed PLL/Alg PEMs. Thus, it is expected that BSA and FN adsorb more tightly after annealing. As already suggested,[22] the viscoelastic

properties of a substrate play a key role in cell adhesion, provided that adhesion proteins that interact with cell integrins are tightly adsorbed to the substrate.

For Chi/HA PEMs, previous data from QCM-D showed limited adsorption of both adhesion (FN) and nonadhesion proteins (BSA).[19] These data are corroborated by the gamma counting results presented in this section, which show that the amount of adsorbed proteins is significantly smaller for Chi/HA PEMs than for PLL/Alg PEMs. This behavior is consistent with the antifouling properties of Chi/HA PEMs reported previously.[19] Moreover, Chi/HA PEMs exhibit a different behavior from that observed for PLL/Alg, which is reflected in decreased cell adhesion for Chi/HA PEMs and enhanced adhesion for PLL/Alg.

2.3. AFM Measurements of Adhesion Proteins on n-PLL/Alg and a-PLL/Alg

Atomic force microscopy is a valuable technique to study the changes in the topography of PEMs and to evaluate distinctive protein structures and organization on surfaces.[39] Unannealed PLL/Alg PEMs exhibited a fibrillar network topography by AFM, with the average length of the fibers being close to 40 nm (**Figure 4**a). Upon annealing, the fibrillar characteristics smear out, and the surface becomes grainy, with grains of about 30 nm in size (Figure 4b). At this length scale, the roughness remains unchanged within the range of experimental error at 1.36 ± 0.08 nm for unannealed PEMs and 1.33 ± 0.05 for annealed PEMs.

When FN is adsorbed for 45 min, AFM measurements in HEPES buffer allow us to distinguish differences in topography for both unannealed (Figure 4c) and annealed PEMs (Figure 4d) compared with samples without FN (Figure 4a,b). For unannealed samples, a decrease in roughness to 1.11 ± 0.05 nm is observed after FN adsorption. Protrusions of about 3–5 nm high and 0.05 µm long, as well as chains of 0.1 µm long could be distinguished (Figure 4c). These changes in surface characteristics confirm the adsorption of FN to the PEM.

On the other hand, the adsorption of FN to annealed PLL/Alg PEMs (Figure 4d) exhibited a more abrupt decrease in roughness from 1.33 to 0.66 nm. As for unannealed PEMs, protrusions of 4–5 nm in height and 0.05 µm in length, and rather smeared out chains were observed (Figure 4f). Data seem to indicate a larger extension of FN adsorption and possibly a change in its structure, compared with unannealed PEMs. Roughness profiles allow us to better distinguish the characteristic features of each sample (Figure 4g–j). Thus, n-PLL/Alg and a-PLL/Alg with absorbed FN show significant differences in topographic features in comparison with samples incubated only in HEPES. For the former, an increase in the peak width and the appearance of local roughness that modulate the profile can be distinguished. For a-PLL/Alg PEMs with FN, the presence of tiny agglomerates is noticeable. Topography appears to

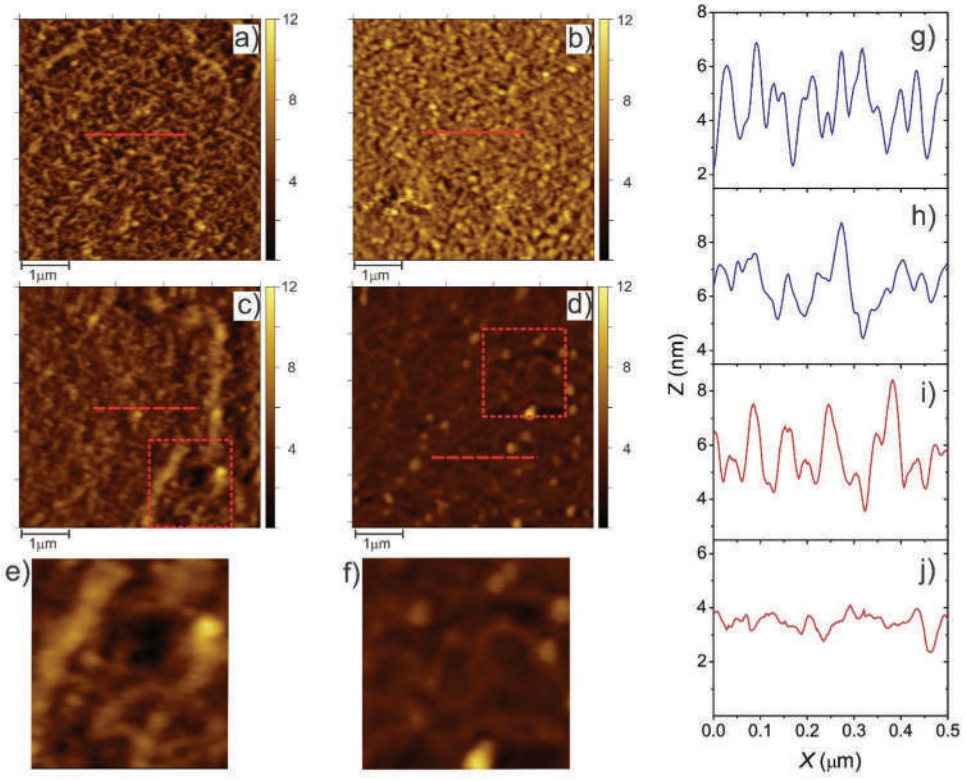

Figure 4. AFM images measured in HEPES buffer of unannealed and annealed PLL/Alg PEMs alone and following adsorption of FN from a 10 µg mL^{-1} FN solution for 45 min. a) n-PLL/Alg, b) a-PLL/Alg, c) n-PLL/Alg with adsorbed FN, and d) a-PLL/Alg with adsorbed FN. e,f) Enlarged images of the region enclosed in the dashed square depicted in (c) and (d), respectively. Typical roughness profiles extracted from the AFM images where indicated by the dashed lines are shown for g) n-PLL/Alg, i) a-PLL/Alg, h) n-PLL/Alg with adsorbed FN, and j) a-PLL/Alg with adsorbed FN.

be globally much smoother and more compact than for n-PLL/Alg. These observations hint to a different arrangement of FN deposited onto the PEMs whether annealed or not, regardless of the secondary structure of the protein, which is analyzed in the next section by circular dichroism (CD) measurements.

FN is a flexible dimeric glycoprotein, with each chain formed by three domains each pertaining a different charge.[40] The extreme domains of FN display charges of −6.6 and −4.2 (elemental charge units) and the central domain a charge of −0.3. Thus, on a negatively charged surface, as is the case for a-PLL/Alg,[18,21] the more stable configuration would involve the FN horizontally oriented with the central domain approaching the surface of the substrate to minimize electrostatic repulsions. This configuration makes the adhesive RGD motif of FN more easily exposed for interacting with cell integrins.[38]

2.4. Circular Dichroism Measurements

CD is used to study the secondary structure of proteins in solution or adsorbed to a substrate.[41–44] CD measurements were performed here on BSA and FN in solution and adsorbed to PLL/Alg PEMs to study the impact of annealing of the PEMs on the secondary structure of the adsorbed proteins (**Figure 5**).

For BSA, a decrease in the percentage of α-helix component was detected upon interaction with either n-PLL/Alg or a-PLL/Alg substrates (Figure 5a,b). A comparison of BSA adsorption data on a-PLL/Alg and n-PLL/Alg indicates that there is a smaller decrease in the α-helix component when adsorbed on a-PLL/Alg than on n-PLL/Alg. This agrees with similar observations by others[45] that better cell adhesion characteristics are obtained for surfaces with a relatively high α-helix component of serum proteins.

It has been reported that the interaction of proteins with surfaces largely affects the β-sheet secondary structure rather than the α-helix.[46] FN in solution exhibited a typical CD spectrum for this protein, with a predominately β-sheet secondary structure (close to 92%, Figure 5c,d). Upon annealing, the β-sheet component decreases but remains high at close to 60%. A closer observation of the CD data reveals that for FN adsorbed to PLL/Alg, the β-sheet component is higher than for BSA and is similar for both annealed and unannealed

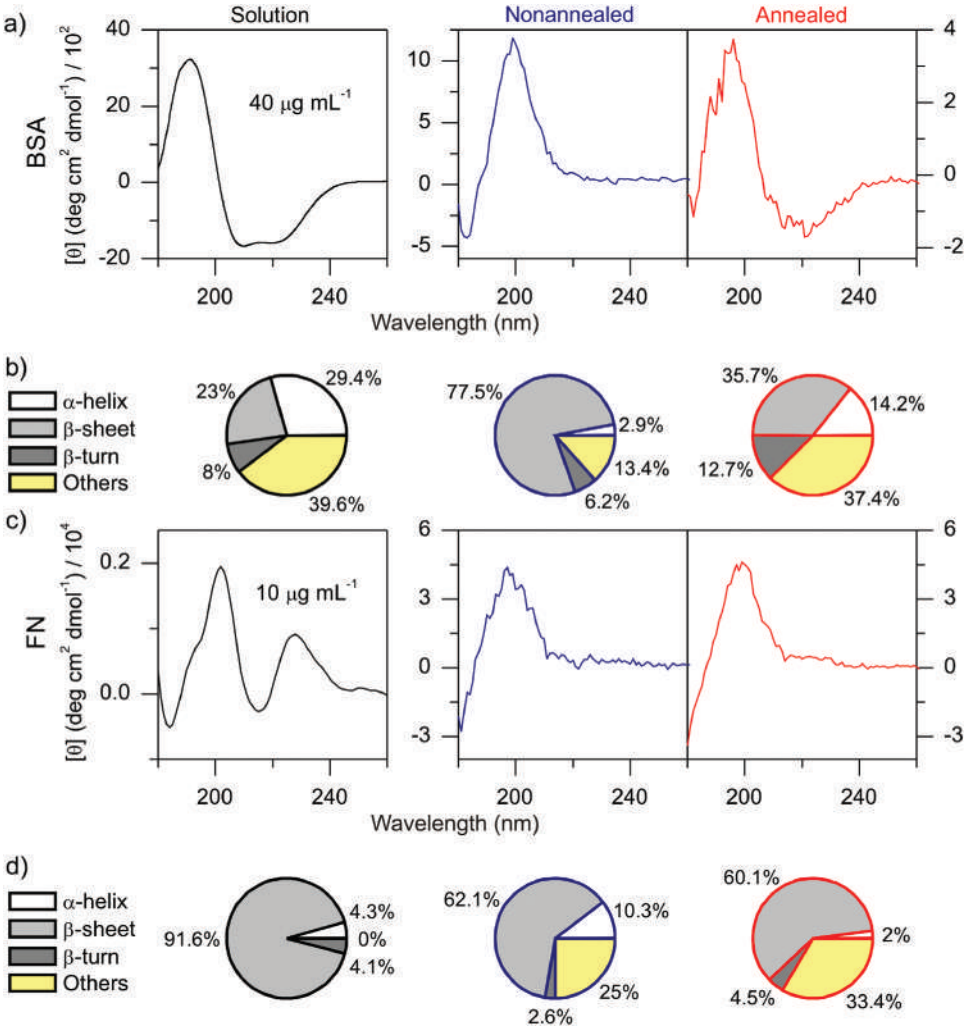

Figure 5. CD spectra and secondary structure content of a,b) BSA and c,d) FN in HEPES solution, or adsorbed to n-PLL/Alg or a-PLL/Alg.

substrates (Figure 5b,d). Changes in the β-type structure contributions (β-sheet or β-turn) were observed, although additional statistics would be needed to determine their significance. We hypothesize that a change in the 3D structure of FN adsorbed either to n-PLL/Alg or a-PLL/Alg would play a key role in the protein adsorption processes as described in the previous subsection.

When BSA is adsorbed to substrates, there is an increase in the β-sheet component of its secondary structure. Conversely, when FN (a typical model β-protein) is adsorbed, a decrease of about 25% in the β component is observed.

3. Discussion

Our results provide a more rational explanation for the enhanced cell adhesion of annealed PLL/Alg PEMs, based on a tighter interaction of proteins with the PEMs after annealing. This increased interaction is reflected in the decrease in the exchangeability of adhesion proteins adsorbed either in contact with the surface substrate, or mediated by nonadhesion, tightly attached BSA layers. It is well known that cell adhesion is promoted by a relatively large amount of nonadhesion proteins cooperating with adhesion proteins, which are present in a much smaller amount.[47] The changes in the physicochemical properties of PEMs upon annealing[18–20] affect the protein–substrate interaction. The increase in the hydrophobicity and the higher density of negative moieties on the interface would induce the change in protein structure, particularly for FN adsorbed on a-PLL/Alg PEMs. A tighter binding of the protein to the PLL/Alg-based PEM is proved by the exchangeability experiments by gamma counting, and the CD results that hint to changes in the FN tertiary structure as the β component remains high regardless of whether PEMs are unannealed or annealed. Changes in the tertiary FN structure with more accessible RGD groups would be driven by the increase in carboxylic group density coming from alginate chains in a-PLL/Alg. It is worth noting that the change in substrate stiffness could also affect protein state as has been reported.[48] Because of these changes in the state of FN on the a-PLL/Alg, a relatively strong interaction of FN with cell membrane integrins resulting in a more effective cell adhesion is observed. Cells are able to expand due to proper forces applied to the substrate for increasing cell cytoplasm tension. In this regard, cells would sense the increase in the substrate's Young's modulus upon annealing. The protein and cell adhesion characteristics to n-PLL/Alg and a-PLL/Alg can be described by a simple scheme (**Figure 6**). Upon annealing, both BSA and FN exhibit an increased interaction with the substrate; moreover, FN adsorbed on a-PLL/Alg adopts an elongated tertiary structure,[40] favoring the exposure of RGD adhesive groups that enhance cell adhesion.

On a-Chi/HA PEMs, an opposite effect was observed from that described for a-PLL/Alg PEMs. FN adheres less tightly to the annealed PEMs as observed by gamma counting. Unlike for PLL/Alg, it was not possible to perform AFM and CD measurements following adsorption due to the low amount of FN deposited on the annealed PEMs, and thus it was not possible to derive conclusions on changes in the packing and conformation of FN. We can only hypothesize that the increase in hydrophilicity and the presence of very narrow fibrils in the PEM after annealing do not facilitate tight attachment of FN to the PEM. BSA deposition is increased after annealing. BSA is a rather large protein, but smaller than FN, with hydrophilic and hydrophobic regions. Upon adsorption, it is likely to modify its structure in a manner different from FN to adhere to the PEMs.[49] As already reported, topographical characteristics would play a key role in cell adhesion.[50] Our results here indicate a combined effect of a larger deposition of BSA, a typical nonadhesion protein, and lower deposition of FN, the latter with an increased exchangeability, which renders the PEM surface unfavorable for stable interactions with integrins from the cell membrane (**Figure 7**). This selectivity in protein adsorption has been previously reported for other systems.[51–53] The selective increase of BSA adsorption upon annealing suggests that the extrapolation of the behavior of

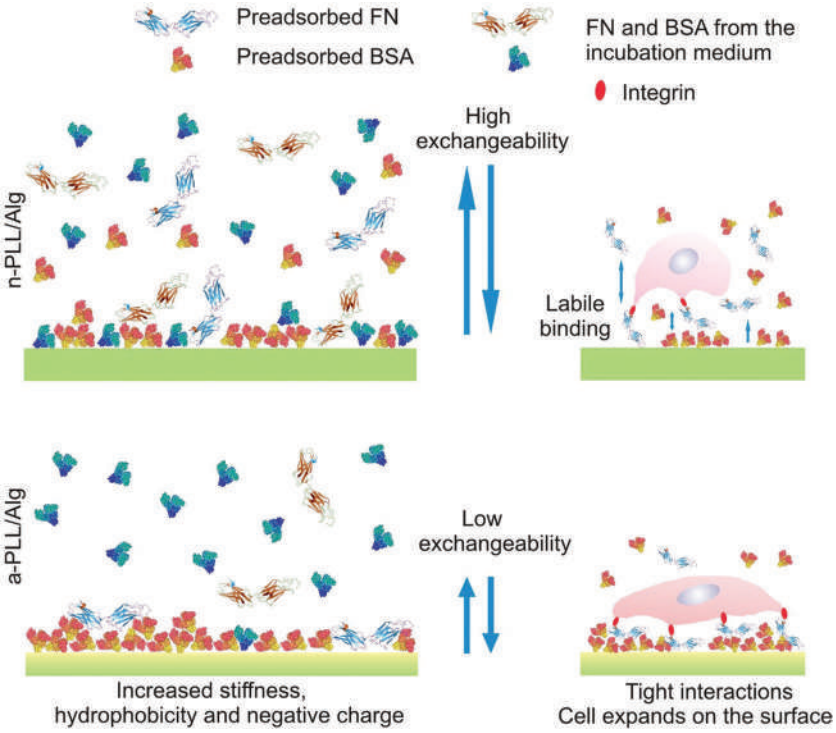

Figure 6. Scheme of protein adhesion mechanism and the effects on cell adhesion characteristics for n-PLL/Alg and a-PLL/Alg. Results from the exchangeability assays are schematically described. On annealed PLL/Alg PEMs, proteins exhibit an augmented interaction with the substrate, the exchangeability is reduced and FN, either alone or in cooperation with BSA, shows a stronger interaction with PEM surfaces. The effect on cell adhesion is also represented. The objects depicted in the scheme are not to scale and for FN, only the FN III fragment is represented.

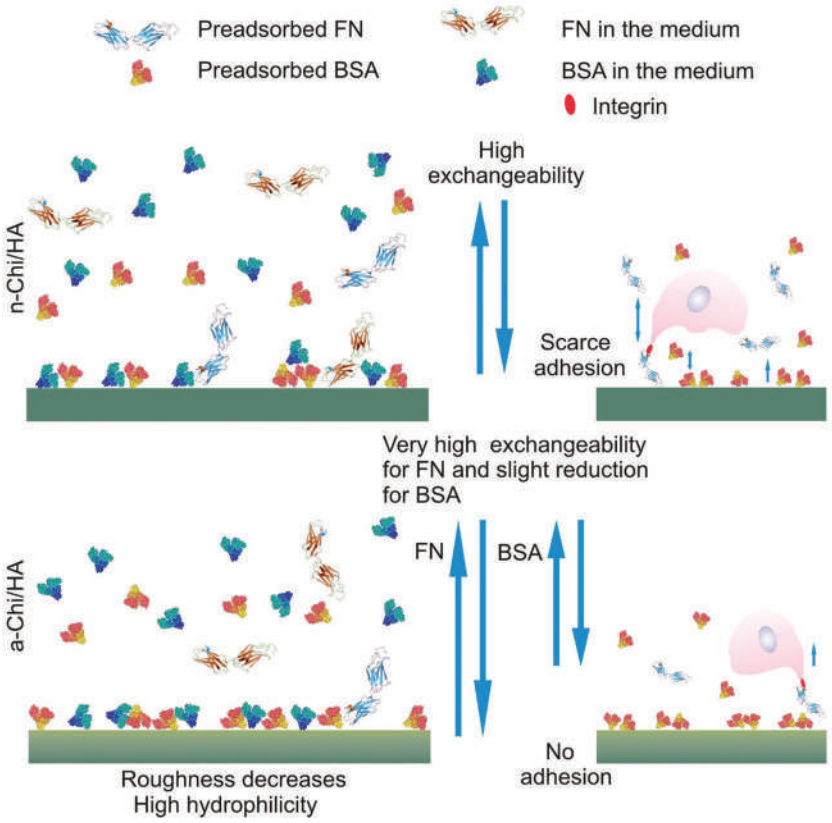

Figure 7. Scheme of protein and cell interactions with n-Chi/HA and a-Chi/HA PEMs. On annealed Chi/HA PEMs the exchangeability assays indicate an increase in the amount and strength of BSA adsorption, and a contrary effect for FN adsorption. Cell adhesion properties are poorer for a-Chi/HA compared with n-Chi/HA. In contrast to PLL/Alg-based PEMs, Chi/HA PEMs do not appear to support cooperation between BSA and FN in the adsorption process.

a protein may induce misleading conclusions about other proteins.

4. Conclusions

We have shown that thermal annealing of PLL/Alg and Chi/HA PEMs has significant consequences on the interaction of the PEM with adhesion and nonadhesion proteins, and through these changes it is possible to explain differences in cell adhesion to PEMs after thermal annealing. Both FN and BSA deposited in larger amounts on the annealed PLL/Alg than on the unannealed PEMs. Moreover, exchangeability experiments with serum-supplemented medium revealed that the proteins were more tightly bound to the annealed PLL/Alg. For a-PLL/Alg, BSA adsorbed from a FN/BSA solution with BSA at a concentration hundredfold higher than FN, affected the interaction of FN with the PEMs and resulted in a cooperative adsorption process. This cooperativity between FN and BSA was not observed for n-PLL/Alg. AFM showed a different packing of FN adsorbed to a-PLL/Alg and n-PLL/Alg, and CD spectroscopy hinted at changes in the secondary structure of FN, a typical β model protein, on both n-PLL/Alg and a-PLL/Alg. For BSA, a smaller decrease in the α-helix component was observed upon adsorption on a-PLL/Alg. For FN, the contribution of its β components decreased upon adsorption but remained high, above 60%. Thus, it is expected that the tertiary structure would be affected. FN molecules are likely to lie onto the surface, minimizing electrostatic repulsion with the negative charge of the a-PLL/Alg. The resulting conformation of FN makes the adhesion motif of the protein more accessible for interaction with cells. The increase in hydrophobicity and the presence of negative charges on a-PLL/Alg would induce the described change in FN deposition. Thus, the annealed PLL/Alg shows higher affinity for FN, and FN molecules arrange in such a way that the interaction with integrins from cells is enhanced. In this scenario, adhesion is improved due to cells sensing the increase in substrate stiffness produced by thermal treatment.

On the contrary, thermal annealing of Chi/HA PEMs increased BSA deposition but decreased the amount of FN molecules attached to the PEMs, which were also less tightly bound, as demonstrated by exchangeability experiments. The combined increase in BSA adsorption and decrease in FN (the latter interacting weaklier with the PEM surface) restricts cell integrins from interacting with the PEMs, which results in limited cell adhesion.

The data presented here provide a rational understanding of cell adhesion on both unannealed and annealed PLL/Alg and Chi/HA PEMs. The model for cell adhesion on PEMs developed based on the adsorption characteristics of model proteins suggests the importance of interfacial protein interactions for assisting cells in sensing changes in the physicochemical properties of the film. Cell/substrate interactions trigger the cascade of events that prompt the cell to expand or retract its cytoskeleton onto the substrate. Understanding the influence that substrate characteristics have on this important process is a fundamental step toward the design of new biocompatible materials for biomedical applications.

5. Experimental Section

Materials and Reagents: PLL solution (MW 70–150 kDa, P4707), sodium chloride, HEPES sodium salt, phosphate buffered saline (PBS, D1408), sodium acetate trihydrate (AcNa, S8625), acetic acid (AcH, 33209), BSA (A7906), FN from human plasma (F1056), sodium dodecadocyl sulfate (SDS, L6026), and Iodo-gen reagent (1,3,4,6-tetrachloro-3α,6α-diphenylglycouril, T0656) were purchased from Sigma-Aldrich. Sodium alginate (Alg, Cat. No. 17777-0050), Chi (MW 100–300 kDa, Cat. No. 349051000), and HA (MW 1500–2200 kDa, Cat. No. 251770010) were acquired from Acros Organics. [^{131}I]-NaI (solution in 0.1 M NaOH) was purchased from Perkin Elmer.

The RPMI 1640 with L-glutamine was purchased from Lonza and FBS from Fisher. Nanopure water was obtained using the Barnstead Nanopure Ultrapure Water Purification System.

Multilayer Film Preparation via LbL Assembly: PLL and Alg solutions were prepared in a 150×10^{-3} M NaCl, 10×10^{-3} M HEPES pH = 7.4 buffer (HEPES buffer). Chi and HA solutions were prepared in a 150×10^{-3} M NaCl, 10×10^{-3} M acetate buffer adjusted to pH 5.0 (acetate buffer). All polyelectrolyte solutions were prepared at a concentration of 1 mg mL^{-1} with the exception of PLL, which was prepared at 0.01 mg mL^{-1}. All solutions were filtered through a 0.45 µm filter. These conditions were selected to assure PEM assembly for the chosen polycation/polyanion combinations.

Glass substrates were cleaned before use as reported previously.[54,55] Briefly, the glasses were immersed in 10×10^{-3} M SDS for 3 h, rinsed in sterile water three times, treated with 0.1 M HCl overnight and thoroughly rinsed in water. For all PEMs shown here, 15 layers of polyelectrolytes were assembled, with the first and the last layer always being a polycation (Figure 1a). Polycations and polyanions were alternately assembled by manual dipping at 24 °C and were allowed to assemble for 15 min. After deposition of each layer, PLL/Alg or Chi/HA films were rinsed three times in water or acetate buffer, respectively. PEMs were UV-sterilized for 1 h in the laminar flow hood and dried before use.[56]

Multilayer Film Annealing: PEMs prepared as described in the previous section (unannealed $(PLL/Alg)_7PLL$ and unannealed $(Chi/HA)_7Chi$, hereinafter referred to as n-PLL/Alg and n-Chi/HA, respectively) were UV-sterilized for 1 h in the laminar flow hood and left in a Memmert UNE 200-300 oven at 37 °C for 72 h to obtain the annealed $(PLL/Alg)_7PLL$ and annealed $(Chi/HA)_7Chi$ films, hereinafter referred to as a-PLL/Alg and a-Chi/HA, respectively (Figure 1a).

Radiochemistry Assays: The radioiodination of BSA and FN was carried out by electrophilic aromatic substitution of tyrosine residues using the Iodogen reagent as an oxidizing agent to obtain [^{131}I]-BSA or [^{131}I]-FN. In brief, sodium phosphate buffer (0.5 M, pH 7.4), [^{131}I]-NaI solution (2 µL, 18.5 ± 2.0 MBq), and BSA (1 mg mL^{-1} in HEPES buffer, 5 µL) or FN (0.5 mg mL^{-1} in HEPES buffer, 10 µL) were mixed for a total volume of 20 µL. The reagents were introduced into Iodogen precoated plastic tubes and allowed to react for 30 min at room temperature. Then, sodium phosphate buffer solution (250 µL, 0.01 M, pH 7.4) and 1 M NaCl solution were added to quench the reaction. The labeled proteins were separated by size-exclusion chromatography using an Illustra NAP-5 column (GE Healthcare, USA). The eluted solution was collected in fractions of ≈140 µL, and the amount of radioactivity in each fraction was determined using a dose calibrator (Carpintec CRC-25, USA) to select those fractions containing the labeled protein. The samples were stored at 4 °C until use. Labeled proteins were mixed with unlabeled proteins to obtain final concentrations of 1 mg mL^{-1} for BSA and 10 µg mL^{-1} for FN. These concentrations are close to those expected in the FBS-supplemented medium. Moreover, fibronectin solutions with concentrations in the range of 5–10 µg mL^{-1} are often used to promote cell adhesion.[57]

PEMs were dipped into the solutions of radiolabeled proteins for 45 min at 24 °C and then rinsed two times in HEPES buffer. Then, samples were placed in polystyrene tubes and the activity was measured in an automatic gamma counter (2470 Wizard, Perkin Elmer, USA). The specific radioactivity (amount of activity per unit mass) was converted into mass of protein. The protein mass per surface area in µg cm^{-2} or ng cm^{-2} was calculated by dividing the mass of radiolabeled proteins by the area of the glass substrates coated with PEMs. In some experiments, to observe the adsorption of the adhesion protein from complex media, PEMs were incubated in a solution of 1 mg mL^{-1} of BSA and 10 µg mL^{-1} of [^{131}I]-FN. After 45 min of incubation at 24 °C, samples were rinsed twice in HEPES buffer, placed in polystyrene tubes, and the amount of radioactivity was measured.

Protein exchange experiments were performed using RPMI culture media with or without 10% of FBS (plain or FBS-supplemented RPMI medium). PEMs were dipped into solutions of radiolabeled protein for 45 min at 24 °C, rinsed two times with HEPES buffer and activity was measured by gamma counting. Then, the films were immersed in cell media, with or without proteins, for 18 h at 24 °C. After incubation, samples were rinsed two times with HEPES buffer and the amount of radioactivity was measured again to determine the loss of labeled protein following the respective exchange. All radiochemistry assays were performed in triplicate.

Circular Dichroism: CD spectra of films were measured with a Jasco J-815 instrument to trace structural changes of proteins adsorbed to the samples. Measurements were run on samples before and after annealing. For this purpose, PEMs were assembled on both sides of three high-quality quartz slides 1.0×2.5 cm^2 (Electron Microscopy Science, 72250-03), and CD measurements were performed in HEPES buffer before and after adsorption of BSA and FN from solutions in HEPES buffer at 1 mg mL^{-1} and 10 µg mL^{-1}, respectively. For CD measurements, the NaCl in HEPES buffer was replaced by Na_2SO_4 to avoid the strong absorption of chloride ions below 200 nm.[41] Prior to measurements, samples were rinsed gently with water and placed in a parallel arrangement containing the three coated quartz coverslips located in between two other clean quartz slides. This configuration was chosen to increase CD signal from the sample.[58,59] CD measurements were performed in a spectral range from 300 to 180 nm, with a scanning speed of 10 nm min^{-1}, a response time of 4 s, and a bandwidth of 1 nm. Each spectrum was obtained by accumulating 4–16 scans. The instrument was calibrated with (1R) (–)10-camphorsulfonic acid ammonium salt. All measurements were carried out at 24 °C and performed in triplicate (three different sets of PEM-coated quartz slides for each condition). CD spectra were converted from raw ellipticity (θ, mdeg) to mean molar ellipticity per residue ([θ], deg cm^2 dmol^{-1}) and secondary structures were determined using BeStSel.[60,61]

Cell Culture: C2C12, a mouse myoblast cell line, was employed for adhesion studies. Cells were grown in RPMI medium supplemented with 10% FBS and antibiotics, and incubated at 37 °C in a 5% CO_2 humidified atmosphere.

Cells were seeded on glass, and films placed in petri dishes 35 mm in diameter (Greiner) previously UV-sterilized for 1 h. Then, a suspension of 5×10^4 cells in 2 mL culture medium was seeded onto the samples. Phase-contrast images were taken at 24 h employing a Nikon T100 inverted microscope with a CFI flat field ADL 10× objective. Cell adhesion was quantified by measuring the cell area in µm^2.

Acknowledgements

S.E.M. thanks the MAT2017-88752-R Retos project from the Spanish Ministry of Science. J.L. thanks the CTQ2017-87637-R Retos project from the Spanish Ministry of Science. The authors thank the Consejo Nacional de Investigaciones Científicas y Técnicas (CONICET, Argentina) (Grant No. PIP 0602), Agencia Nacional de Promoción Científica y Tecnológica (ANPCyT, Argentina; PICT-163/08, PICT-2010-2554, and PICT-2013-0905), the Austrian Institute of Technology 1GmbH (AIT-CONICET Partner Group: "Exploratory Research for Advanced Technologies in Supramolecular Materials Science," Exp. 4947/11, Res. No. 3911, 28-12-2011), and Universidad Nacional de La Plata (UNLP). M.A.P. and O.A. are staff members of CONICET. This work was performed under the Maria de Maeztu Units of Excellence Program from the Spanish State Research Agency (Grant No. MDM-2017-0720). The authors thank Dr. Julia Cope for her kind revision of the manuscript.

Conflict of Interest

The authors declare no conflict of interest.

Keywords

cell adhesion modulation, fibronectin, polyelectrolyte multilayer, protein adsorption, thermal annealing

Received: January 2, 2019
Revised: January 29, 2019
Published online: February 13, 2019

[1] J. Pizarro-Cerdá, P. Cossart, *Cell* **2006**, *124*, 715.
[2] V. Barone, C.-P. Heisenberg, *Curr. Opin. Cell Biol.* **2012**, *24*, 148.
[3] J. Boateng, O. Catanzano, *J. Pharm. Sci.* **2015**, *104*, 3653.
[4] G. Bendas, L. Borsig, *Int. J. Cell Biol.* **2012**, *2012*, 1.
[5] S. Guo, X. Zhu, *Mater. Sci. Eng., C* **2017**, *70*, 1163.
[6] M. Ventre, P. A. Netti, *ACS Appl. Mater. Interfaces* **2016**, *8*, 14896.
[7] J. Schaller, *Human Blood Plasma Proteins: Structure and Function*, Wiley, New York **2008**.
[8] Y. Arima, H. Iwata, *Acta Biomater.* **2015**, *26*, 72.
[9] K. Minami, Y. Kasuya, T. Yamazaki, Q. Ji, W. Nakanishi, J. P. Hill, H. Sakai, K. Ariga, *Adv. Mater.* **2015**, *27*, 4020.
[10] A. J. Engler, S. Sen, H. L. Sweeney, D. E. Discher, *Cell* **2006**, *126*, 677.
[11] J. C. Chen, C. R. Jacobs, *Stem Cell Res. Ther.* **2013**, *4*, 107.
[12] K. Minami, T. Mori, W. Nakanishi, N. Shigi, J. Nakanishi, J. P. Hill, M. Komiyama, K. Ariga, *ACS Appl. Mater. Interfaces* **2017**, *9*, 30553.
[13] B. L. Li, M. I. Setyawati, L. Chen, J. Xie, K. Ariga, C.-T. Lim, S. Garaj, D. T. Leong, *ACS Appl. Mater. Interfaces* **2017**, *9*, 15286.
[14] G. Decher, *Science* **1997**, *277*, 1232.
[15] T. Crouzier, T. Boudou, C. Picart, *Curr. Opin. Colloid Interface Sci.* **2010**, *15*, 417.
[16] V. Gribova, R. Auzely-Velty, C. Picart, *Chem. Mater.* **2012**, *24*, 854.
[17] R. R. Costa, J. F. Mano, *Chem. Soc. Rev.* **2014**, *43*, 3453.
[18] N. E. Muzzio, D. Gregurec, E. Diamanti, J. Irigoyen, M. A. Pasquale, O. Azzaroni, S. E. Moya, *Adv. Mater. Interfaces* **2017**, *4*, 1600126.
[19] N. E. Muzzio, M. A. Pasquale, E. Diamanti, D. Gregurec, M. Martinez Moro, O. Azzaroni, S. E. Moya, *Mater. Sci. Eng., C* **2017**, *80*, 677.
[20] N. E. Muzzio, M. A. Pasquale, S. E. Moya, O. Azzaroni, *Biointerphases* **2017**, *12*, 04E403.
[21] E. Diamanti, N. Muzzio, D. Gregurec, J. Irigoyen, M. Pasquale, O. Azzaroni, M. Brinkmann, S. E. Moya, *Colloids Surf., B* **2016**, *145*, 328.
[22] C. J. Arias, R. L. Surmaitis, J. B. Schlenoff, *Langmuir* **2016**, *32*, 5412.
[23] Q. Wei, T. Becherer, S. Angioletti-Uberti, J. Dzubiella, C. Wischke, A. T. Neffe, A. Lendlein, M. Ballauff, R. Haag, *Angew. Chem., Int. Ed.* **2014**, *53*, 8004.
[24] H. M. Kowalczyńska, M. Nowak-Wyrzykowska, R. Kołos, J. Dobkowski, J. Kamiński, *J. Biomed. Mater. Res., Part A* **2005**, *72A*, 228.
[25] H. M. Kowalczynńska, M. Nowak-Wyrzykowska, R. Kołos, J. Dobkowski, J. Kaminński, *J. Biomed. Mater. Res., Part A* **2008**, *87A*, 944.
[26] C. F. Wertz, M. M. Santore, *Langmuir* **2001**, *17*, 3006.
[27] C. C. Barrias, M. C. L. Martins, G. Almeida-Porada, M. A. Barbosa, P. L. Granja, *Biomaterials* **2009**, *30*, 307.
[28] J. Deng, M. Sun, S. Wang, L. Han, Z. Mao, D. Li, H. Chen, C. Gao, *Macromol. Biosci.* **2015**, *15*, 241.
[29] F. Grinnell, M. K. Feld, *J. Biomed. Mater. Res.* **1981**, *15*, 363.
[30] T. Miller, D. Boettiger, *Langmuir* **2003**, *19*, 1723.
[31] H. M. Kowalczyńska, M. Nowak-Wyrzykowska, *Cell Biol. Int.* **1999**, *23*, 359.
[32] H. M. Kowalczyńska, M. Nowak-Wyrzykowska, *Cell Biol. Int.* **2003**, *27*, 101.
[33] M. H. Lee, P. Ducheyne, L. Lynch, D. Boettiger, R. J. Composto, *Biomaterials* **2006**, *27*, 1907.
[34] U. Jönsson, B. Ivarsson, I. Lundström, L. Berghem, *J. Colloid Interface Sci.* **1982**, *90*, 148.
[35] B. G. Keselowsky, D. M. Collard, A. J. García, *J. Biomed. Mater. Res., Part A* **2003**, *66A*, 247.
[36] Y. Arima, H. Iwata, *Biomaterials* **2007**, *28*, 3074.
[37] M. Kopecek, L. Bacakova, J. Vacik, F. Fendrych, V. Vorlicek, I. Kratochvilova, V. Lisa, E. Van Hove, C. Mer, P. Bergonzo, M. Nesladek, *Phys. Status Solidi A* **2008**, *205*, 2146.
[38] G. Kerch, *Nanomed.: Nanotechnol., Biol. Med.* **2018**, *14*, 13.
[39] M. Bergkvist, J. Carlsson, S. Oscarsson, *J. Biomed. Mater. Res.* **2003**, *64A*, 349.
[40] A. P. Ngankam, G. Mao, P. R. Van Tassel, *Langmuir* **2004**, *20*, 3362.
[41] S. M. Kelly, T. J. Jess, N. C. Price, *Biochim. Biophys. Acta, Proteins Proteomics* **2005**, *1751*, 119.
[42] N. J. Greenfield, *Nat. Protoc.* **2007**, *1*, 2876.
[43] M. Rabe, D. Verdes, S. Seeger, *Adv. Colloid Interface Sci.* **2011**, *162*, 87.
[44] W. Norde, C. E. Giacomelli, *J. Biotechnol.* **2000**, *79*, 259.
[45] A. Hasan, S. K. Pattanayek, L. M. Pandey, *ACS Biomater. Sci. Eng.* **2018**, *4*, 3224.
[46] E. Osterlund, I. Eronen, K. Osterlund, M. Vuento, *Biochemistry* **1985**, *24*, 2661.
[47] J. E. Koblinski, M. Wu, B. Demeler, K. Jacob, H. K. Kleinman, *J. Cell Sci.* **2005**, *118*, 2965.
[48] J.-H. Seo, K. Sakai, N. Yui, *Acta Biomater.* **2013**, *9*, 5493.
[49] K. P. Fears, C. T. Love, D. E. Day, *Biointerphases* **2017**, *12*, 02D403.
[50] M. S. Lord, M. Foss, F. Besenbacher, *Nano Today* **2010**, *5*, 66.
[51] G. Anand, F. Zhang, R. J. Linhardt, G. Belfort, *Langmuir* **2011**, *27*, 1830.
[52] H. P. Felgueiras, N. S. Murthy, S. D. Sommerfeld, M. M. Brás, V. Migonney, J. Kohn, *ACS Appl. Mater. Interfaces* **2016**, *8*, 13207.
[53] I. Han, B. Vagaska, B. J. Park, M. H. Lee, S. J. Lee, J. C. Park, *J. Appl. Phys.* **2011**, *109*, 124701.
[54] A. L. Hillberg, C. A. Holmes, M. Tabrizian, *Biomaterials* **2009**, *30*, 4463.
[55] N. E. Muzzio, M. A. Pasquale, D. Gregurec, E. Diamanti, M. Kosutic, O. Azzaroni, S. E. Moya, *Macromol. Biosci.* **2016**, *16*, 482.
[56] L. Han, Z. Mao, J. Wu, Y. Guo, T. Ren, C. Gao, *Biomaterials* **2013**, *34*, 975.
[57] J.-L. Guan, *Signaling through Cell Adhesion Molecules*, CRC Press, Boca Raton, FL **1999**.
[58] B. Sivaraman, K. P. Fears, R. A. Latour, *Langmuir* **2009**, *25*, 3050.
[59] K. P. Fears, D. Y. Petrovykh, S. J. Photiadis, T. D. Clark, *Langmuir* **2013**, *29*, 10095.
[60] A. Micsonai, F. Wien, L. Kernya, Y.-H. Lee, Y. Goto, M. Réfrégiers, J. Kardos, *Proc. Natl. Acad. Sci. USA* **2015**, *112*, E3095.
[61] A. Micsonai, F. Wien, É. Bulyáki, J. Kun, É. Moussong, Y.-H. Lee, Y. Goto, M. Réfrégiers, J. Kardos, *Nucleic Acids Res.* **2018**, *46*, W315.